

# The application of a VUV Fourier transform spectrometer and synchrotron radiation source to measurements of: II. The $\delta(1,0)$ band of NO

T. Imajo

*Kyushu University, Fukuoka 812, Japan*

K. Yoshino, J. R. Esmond, and W. H. Parkinson

*Harvard-Smithsonian Center for Astrophysics, Cambridge, Massachusetts 02138*

A. P. Thorne, J. E. Murray, R. C. M. Learner, and G. Cox

*Blackett Laboratory, Imperial College, London SW7-2BZ, United Kingdom*

A. S.-C. Cheung

*The University of Hong Kong, Hong Kong*

K. Ito and T. Matsui<sup>a)</sup>

*Photon Factory, KEK, Tsukuba, Ibaraki 305, Japan*

(Received 7 October 1999; accepted 4 November 1999)

Line-by-line photoabsorption cross-sections of the NO  $\delta(1,0)$  band were measured with the VUV Fourier transform spectrometer from Imperial College, London, using synchrotron radiation at Photon Factory, KEK, Japan, as a continuum light source. The analysis of the NO  $\delta(1,0)$  band provides accurate rotational line positions and term values as well as the photoabsorption cross-sections. The molecular constants of the  $C(1)^2\Pi$  level are found to be  $T_0 = 54\,690.155 \pm 0.03 \text{ cm}^{-1}$ ,  $B_v = 1.944\,06 \pm 0.000\,62 \text{ cm}^{-1}$ ,  $D_v = (5.91 \pm 0.42) \times 10^{-5} \text{ cm}^{-1}$ ,  $A_D = -0.0187 \pm 0.0050 \text{ cm}^{-1}$ ,  $p = -0.0189 \pm 0.0037 \text{ cm}^{-1}$ , and  $q = -0.015\,21 \pm 0.000\,20 \text{ cm}^{-1}$ . The sum of the line strengths for all rotational transitions of the NO  $\delta(1,0)$  band is determined as  $4.80 \times 10^{-15} \text{ cm}^2 \text{ cm}^{-1}$ , corresponding to a band oscillator strength of  $0.0054 \pm 0.0003$ . © 2000 American Institute of Physics. [S0021-9606(00)00805-9]

## I. INTRODUCTION

Molecular absorption of ultraviolet solar radiation in the middle atmosphere has been discussed by a number of authors.<sup>1-4</sup> In the wavelength region 175–205 nm the penetration of solar radiation into the atmosphere is controlled by the absorption cross-sections of the Schumann–Runge (SR) bands of O<sub>2</sub>. Part of the radiation transmitted is available to photopredissociate NO, which has a number of strong bands with very narrow lines in the region 183–195 nm. The photodestruction of O<sub>2</sub> and NO is recognized as important stratospheric processes, and their evaluation requires accurate knowledge of the rotational structure of the band systems. For accurate modeling of the processes the computations must be performed on a line-by-line basis: photoabsorption cross-sections, measured in the laboratory with resolution sufficient to yield true cross-sections, are required for both molecules. For most of the SR bands of <sup>16</sup>O<sub>2</sub> such high resolution measurements have been completed and the results incorporated in models of O<sub>2</sub> transmissions and photolysis (e.g., Nicolet and Kennis,<sup>5</sup> Minschwaner *et al.*<sup>6</sup>).

The NO lines are considerably sharper than the O<sub>2</sub> SR lines. Published integrated cross-sections<sup>7-9</sup> measured at insufficient spectral resolution in some cases differ by more than 50%; the differences could indicate that some of the measurements were plagued by saturation, which is very difficult to detect when linewidths are much narrower than the

instrument widths.<sup>10</sup> To overcome the problems of insufficient resolution, line-by-line measurements of the absorption cross-sections of the  $\delta(0,0)$  and  $\beta(7,0)$  bands of NO in the region 195–183 nm were performed by Murray *et al.*<sup>11</sup> using the Fourier transform (FT) spectrometers at Imperial College, London, (IC) with a resolution of  $0.06 \text{ cm}^{-1}$ . A positive-column hydrogen discharge at high current ( $\sim 500 \text{ mA}$ ) was used for a background continuum, with a 0.3 m Czerny–Turner spectrometer (McPherson model 218) to limit the bandwidth to 1 to 2 nm. A signal-to-noise (S/N) ratio of 25 was achieved by coadding up to 128 runs, but this was not sufficient to determine the photoabsorption cross-sections of weaker lines accurately. Because the signal-to-noise ratio achieved was close to the expected photon noise limit, it could be significantly improved only by using a brighter background continuum light source, such as synchrotron radiation.

Recently we combined high-resolution VUV Fourier transform spectrometry with synchrotron radiation by taking the IC VUV FT spectrometer, to the synchrotron radiation source at Photon Factory, KEK, Japan, where a suitable zero dispersion two-grating predisperser is available on beam line 12-B. (The predisperser is necessary to limit the bandwidth to a few nm in order to achieve acceptable S/N ratios.) We have used this combination of facilities to make ultra high resolution cross-section measurements of NO and O<sub>2</sub> bands in the wavelength region 195–160 nm. Results for the  $\beta(9,0)$  ( $B^2\Pi_r - X^2\Pi_r$ ) band of NO have recently been reported by

<sup>a)</sup>Present address: HSRC, Hiroshima University, Hiroshima 739, Japan.

Yoshino *et al.*<sup>12</sup> The present article presents the spectroscopic analysis and the line and band oscillator strengths of the  $\delta(1,0)$  ( $C^2\Pi_r-X^2\Pi_r$ ) band of NO.

The close coincidence of the  $v=0$  level of  $C(v)^2\Pi$  with the first dissociation energy of NO results in predissociation by interaction with the  $a^4\Pi$  continuum.<sup>13,14</sup> Predissociation has been confirmed by radiative lifetime measurements of the  $C(0)$  rotational levels: a sudden change of the lifetime of the rotational levels was measured, from around 25 ns for low  $J$  to 1 ns for high  $J$ .<sup>15-17</sup> Attempts have also been made to measure the lifetime of the  $C(1)$  level, which is very short, in the range of 0.03 to 0.4 ns.<sup>15,18,19</sup> Amiot and Verges<sup>20</sup> performed emission studies of the  $D-A$  and  $C-A$  bands at high resolution,  $0.007\text{ cm}^{-1}$ , with an infrared Fourier transform (IR FT) spectrometer. They observed the  $C(1)-A(1)$  band for the first time in emission, with broad rotational lines indicating predissociation of the  $C(1)$  level. The intensity and linewidth studies have not been published.<sup>21</sup>

The cross-section measurements of the  $C(1)-X(0)$  band by Bethke<sup>7</sup> were performed at low resolution,  $0.04\text{ nm}$ , in the presence of Ar. The rotational lines were pressure-broadened to well beyond the instrumental width, enabling the true cross-sections to be measured. Callear and Pilling<sup>13</sup> suggested that the results for the delta bands might be in error because the collision broadening is different for lines that are predissociated and lines that are not. Cieslik<sup>8</sup> made low resolution measurements of NO at low pressure and used the equivalent width and curve of growth to obtain the band oscillator strength of the  $\delta(1,0)$  band and obtained a result in good agreement with Bethke's. Guest and Lee<sup>9</sup> used a synchrotron source and resolution of  $0.03\text{ nm}$  with very low pressures of NO ( $2 \times 10^{-4}\text{ Torr}$ ). Their result for the  $\delta(1,0)$  band is 48% higher than Bethke's. Chan *et al.*<sup>22</sup> used the high resolution dipole ( $e, e$ ) technique, which is not sensitive to the instrumental resolution. Their value of the oscillator strength of the  $\delta(1,0)$  band agrees with Bethke's.

## II. EXPERIMENT

Details of the experimental setup were described in our previous article.<sup>12</sup> The synchrotron radiation transmitted by the zero-dispersion predisperser in the 12-B beam line of the Photon Factory was reflected by a cylindrical mirror and focused onto the entrance aperture of the FT spectrometer. The center wavelength and bandwidth of the transmitted radiation were set at 185 and 2 nm, respectively to cover the  $\delta(1,0)$  band of NO. The IC VUV spectrometer is equipped with a beam splitter made from a single crystal of  $\text{MgF}_2$ .<sup>23</sup> The spectral resolution of the FT spectrometer was  $0.06\text{ cm}^{-1}$ , requiring an entrance aperture of 1.5 mm diameter. The absorption cell, with an optical path length of 0.565 cm, was placed between the predisperser and the FT spectrometer, and NO gas was introduced at a pressure of 0.4 Torr, corresponding to a column density of  $7.40 \times 10^{15}\text{ mol cm}^{-2}$ . The NO pressure was measured with a capacitance manometer (MKS Baratron). In this case we coadded 320 scans, corresponding to about 14 h integration time. The S/N ratio in the continuum background was 96. Another spectrum was recorded at the same optical path length with a different NO

pressure, 0.2 Torr, in order to estimate the error in pressure measurements. For this spectrum we coadded 160 scans, and the S/N ratio in the continuum background was 59. In addition, a measurement with an optical path length of 0.28 cm and NO pressure of 0.314 Torr was made, yielding a S/N ratio of 72 after coadding 224 scans. The column densities of these two measurements were  $3.70 \times 10^{15}$  and  $2.92 \times 10^{15}\text{ mol cm}^{-2}$ , respectively.

## III. ANALYSIS OF THE SPECTRUM

### A. Fitting of the FTS data

The transmission spectra were converted to optical depth by taking the logarithms of the intensity and fitting a smooth continuum to the regions between the lines. The absorption lines were fitted to Voigt profiles using the spectral reduction routine GREMLIN.<sup>24</sup> Line parameters are determined through a nonlinear least-squares iterative procedure. The Voigt profile for the NO lines should be a convolution of a Gaussian due to Doppler broadening and a Lorentzian arising from predissociation. In this case the Gaussian component of the best fit Voigt function had a full width at half maximum (FWHM) of  $0.175\text{ cm}^{-1}$  which is significantly larger than the value of  $0.12\text{ cm}^{-1}$  expected for Doppler width in our experimental conditions. This anomalous Gaussian width is considered to be due to drifts in alignment causing very small wave number shifts over the long observation periods.<sup>25</sup>

### B. Rotational term values of the $C(1)$ level

The  $\delta(1,0)$  band is shown in Fig. 1(a), and a portion of the spectrum is expanded in Fig. 1(b) to show the detail of the rotational structure. We observed 201 lines, and these lines are assigned in Table I to 235 rovibronic transition of  $C^2\Pi(v=1)-X^2\Pi(v=0)$  according to the results of Lagerqvist and Miescher.<sup>26</sup> Three lines of the  $Q_{11}(J)$  and  $Q_{22}(J)$  branches were assigned in the present work for the first time. Although the majority of the lines are separated, about one-third of them are blended with lines from other branches or from the same branch with a different  $J$  quantum number. These are marked with a B or b following the wave numbers in the table. Blended lines followed by B were treated as a single line, while line positions followed by b were extracted by a deconvolution procedure for an incompletely resolved complex. At least one reference wave number is needed for absolute calibration in FT spectroscopy. The resonance line of Hg I at 184.8 nm was used as reference wave number in our previous article.<sup>12</sup> In this wavelength region we have no convenient absolute reference. However, there is a small overlap between the two spectra, from which we can derive a calibration constant for the present spectrum with an uncertainty of  $0.02\text{ cm}^{-1}$ . Relative uncertainties for the strong lines are better than  $0.01\text{ cm}^{-1}$ . Differences in the observed line positions between our results and Lagerqvist and Miescher<sup>26</sup> are plotted in Fig. 2. They claimed an uncertainty in their line positions of  $0.1\text{ cm}^{-1}$  which is consistent with the results shown in Fig. 2.

The rotational term values of the  $v=1$  level of the  $C^2\Pi_r$  state can be obtained by adding the term values of the  $X(0)$  levels to the wave numbers of the observed lines. The

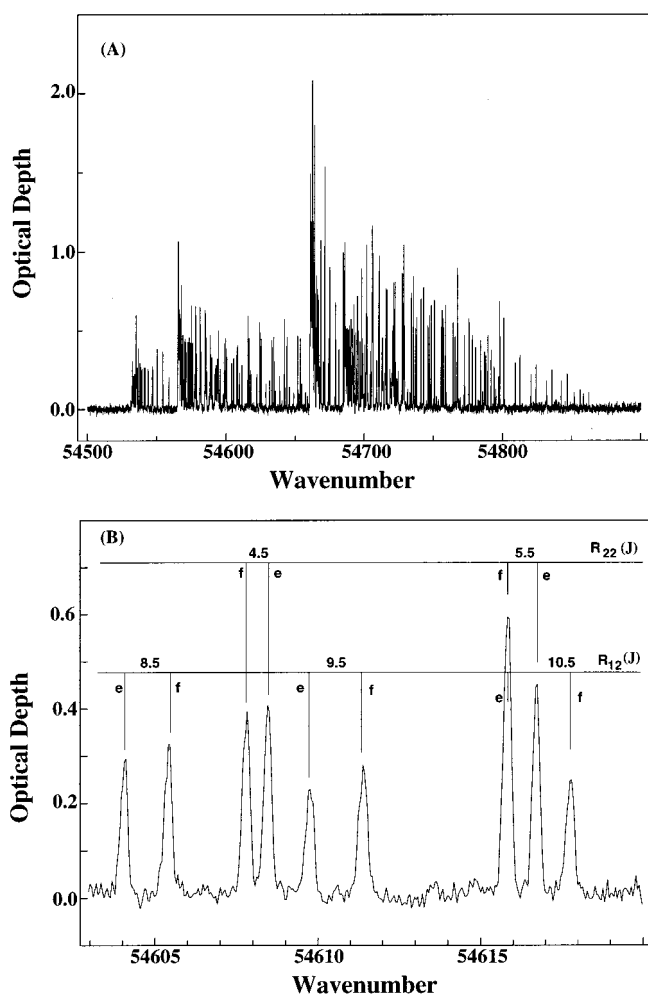


FIG. 1. The  $\delta(1,0)$  band at 0.400 Torr of NO with 0.565 cm pathlength is shown in Fig. 1(a). A portion of the spectrum is expanded in Fig. 1(b). Separations of the  $\Lambda$ -type doubling are seen in  $R_{12}$  and  $R_{22}$  branch lines.

rotational term values of the  $X(0)$  levels relative to the level  $\Omega = \frac{1}{2}$ ,  $J=0.5$ ,  $e$  are given by Amiot *et al.*<sup>27</sup> Our term values are obtained by averaging over the branch lines. The term values recorded from the three spectra at different column densities coincided within  $0.05 \text{ cm}^{-1}$ . The average term values from the three runs are listed in Table II, with the standard deviation shown as an estimated error. The uncertainty in the absolute value of  $T_0$  including the calibration uncertainty is  $0.03 \text{ cm}^{-1}$ .

The effective Hamiltonian operator, suitable for the description of the  $^2\Pi$  states, can be found in Hougen<sup>28</sup> and Zare *et al.*<sup>29</sup> The matrix elements used in this work for the calculation of rotational energy levels are the same as those in Amiot *et al.*<sup>30</sup> and Stark *et al.*<sup>31</sup> The parameters included in the description of the  $^2\Pi$  state are: The band origin  $T_0$ ; the rotational parameters  $B$  and  $D$ ; the spin-orbit parameters  $A$  and  $A_D$ ; and the  $\Lambda$ -doubling parameters  $p$  and  $q$ . In our analysis, we have performed least-squares fittings to the rovibronic term values. The term values corresponding to  $J$  values above 11.5 were not included in the fit because line shifts were expected from perturbation by the  $B(10)$  level. Table II summarizes the molecular constants obtained for the  $v=1$  level of the  $C^2\Pi$  state.

### C. The integrated cross-sections of the $\delta(1,0)$ band

As mentioned before, the absorption lines are fitted to Voigt profiles while the Gaussian contribution is kept constant as  $0.175 \text{ cm}^{-1}$ . The fitting procedure provides integrated cross-sections as well as line positions. These are independent of the anomalous widths, provided that the residuals from the fit are down at the noise level. The integrated cross-sections of blended lines have been separated by using branching ratios observed for other transitions together with the Boltzmann population distribution. The integrated cross-sections of  $R_{11}$  branch lines are plotted in Fig. 3. The lines with  $J>4$  consist of two components,  $e$  and  $f$ , indicated by solid and open circles, respectively. The total cross-sections are represented by the solid squares. These cross-sections are derived from the total column density of NO and therefore depend on the temperature, which was 295 K in this case. The lines belonging to the  $P_{11}$  branch form a bandhead and are strongly overlapped, as indicated by the blending shown in Table I. Hence only the total integrated cross-section is given in Table III. The values listed in Table III can be divided by the fractional populations of the rotational levels to obtain values proportional to the line oscillator strengths. The strengths of the branches are obtained by adding the integrated cross-sections of all rotational lines in the branch. These are listed at the bottom line of Table III.

The uncertainties in the integrated cross-sections are due to noise and to errors in the measurement of the NO pressure and optical path length. Because the cross-sections from the same optical path length 0.565 cm with two different NO pressures coincided well, the error in the pressure measurements was considered small. However, cross-sections from the shorter path 0.284 cm deviated by as much as 40% from those with the longer path 0.565 cm. The discrepancy is believed to be due to uncertainty in the length of the shorter path, and therefore the cross-sections from this path were not included in the calculation of the averaged value of the cross-sections. The differences between the other two data sets with the same path length were compatible with the noise level. The photon noise in FT spectroscopy is virtually constant throughout the spectrum, and in our experiments it amounted typically to an uncertainty for a single point in the cross-section of  $\pm 1.70 \times 10^{-18} \text{ cm}^2$  for lines that are on the linear part of the curve of growth; the uncertainty for partly saturated lines is rather greater. The uncertainty for a strong unblended line of integrated cross-section  $3 \times 10^{-17} \text{ cm}^2 \text{ cm}^{-1}$  is 5.6%. For weak lines of integrated cross-section  $2 \times 10^{-17}$  and  $1 \times 10^{-17} \text{ cm}^2 \text{ cm}^{-1}$  the uncertainties are 9% and 17%, respectively. As the integrated band strength is determined predominantly by the strong lines, we ascribe an error of 6% to this. For all branches the integrated cross-sections were found to be a smooth function of  $J$  which reflects the Boltzmann distribution in the ground state, but several unexpectedly large integrated cross-sections were obtained at  $R_{22}(12.5)_e$  and  $P_{21}(12.5)_e$ . The reason for these large integrated cross-sections is not understood.

The band oscillator strength of a  $(v', v'')$  band is given by

TABLE I. Observed wavenumbers of the  $\delta(1,0)$  band of NO.<sup>a</sup>

$J$	$R_{11}(J)_e$	$R_{11}(J)_f$	$R_{12}(J)_e$	$R_{12}(J)_f$	$R_{21}(J)_e$	$R_{21}(J)_f$	$R_{22}(J)_e$	$R_{22}(J)_f$
0.5	54 692.738B				54 699.329			
1.5	54 695.189		54 575.273B		54 706.084B		54 586.216	
2.5	54 698.319		54 578.206B		54 713.469	54 713.113	54 593.359	54 593.046
3.5	54 701.994B		54 581.493B		54 721.224	54 720.721B	54 600.750	54 600.265b
4.5	54 706.084B	54 706.522	54 585.110B	54 585.613	54 729.511	54 728.931B	54 608.563	54 607.900
5.5	54 710.818	54 711.320B	54 589.294b	54 589.935b	54 738.282	54 737.324	54 616.818	54 615.928B
6.5	54 715.958B	54 716.721	54 593.886	54 594.701B	54 747.554	54 746.348	54 625.472	54 624.400B
7.5	54 721.628	54 722.619	54 598.833B	54 599.915b	54 757.345	54 755.840	54 634.543	54 633.141
8.5	54 727.749	54 728.931	54 604.163	54 605.519	54 767.455B	54 765.772	54 643.994	54 642.290B
9.5	54 734.345	54 735.896	54 609.858	54 611.506	54 778.280	54 776.135	54 653.799	54 651.749
10.5	54 741.355	54 743.216	54 615.928B	54 617.871	54 789.389	54 786.862	54 664.011B	54 661.474B
11.5	54 748.746	54 750.947	54 624.400B	54 624.400B	54 800.787	54 797.880B	54 674.315	54 671.536B
12.5	54 756.472	54 759.030	54 628.812	54 631.501	54 812.526	54 809.231	54 684.945	54 681.720
13.5	54 764.438	54 767.455	54 635.567	54 638.624	54 824.324	54 820.635	54 695.567B	54 691.904
14.5	54 772.499	54 775.812	54 642.290B	54 645.774	54 835.920	54 831.923	54 706.084B	54 701.994B
15.5	54 780.441	54 784.070	54 652.694	54 648.930	54 846.955	54 842.636	54 715.506	54 711.320B
16.5	54 787.823	54 791.707	54 654.783	54 658.910				
17.5	54 793.859	54 797.880						
18.5	54 797.079	54 800.787						
$J$	$P_{11}(J)_e$	$P_{11}(J)_f$	$P_{12}(J)_e$	$P_{12}(J)_f$	$P_{21}(J)_e$	$P_{21}(J)_f$	$P_{22}(J)_e$	$P_{22}(J)_f$
0.5								
1.5								
2.5	54 679.255		54 559.107		54 685.969B		54 565.749B	
3.5	54 675.104		54 554.621		54 685.969B		54 565.749B	
4.5	54 671.536B		54 550.650		54 687.744	54 687.275	54 565.749B	
5.5	54 688.636B		54 547.151		54 687.780	54 687.266	54 566.353b	54 565.749B
6.5	54 665.994	54 666.340	54 543.893	54 544.340	54 689.391	54 688.639	54 567.314	54 566.660b
7.5	54 664.011B	54 664.512	54 541.186	54 541.808	54 691.482	54 690.506	54 568.679	54 567.760
8.5	54 662.365B	54 663.259	54 538.884	54 539.720	54 694.089	54 692.738B	54 570.484	54 569.347
9.5	54 661.474B	54 662.365B	54 536.972b	54 538.076	54 697.156	54 695.567B	54 572.686	54 571.273
10.5	54 660.840B	54 662.365B	54 535.443B	54 536.785b	54 700.720	54 698.893	54 575.273B	54 573.550
11.5	54 660.840B	54 662.365B	54 534.282	54 535.937B	54 704.726	54 702.553	54 578.206B	54 576.172
12.5	54 661.047B	54 662.979B	54 533.480	54 535.443B	54 709.158	54 706.084B	54 581.493B	54 579.096
13.5	54 662.016	54 664.011B	54 532.960b	54 535.443B	54 713.912	54 711.320B	54 585.110B	54 582.275
14.5	54 662.979B	54 665.459B	54 532.622B	54 535.443B	54 718.919	54 715.958B	54 588.759b	54 585.613
15.5	54 664.011B	54 666.947B			54 724.032	54 720.721B	54 592.516b	54 588.973b
16.5	54 665.459B	54 688.636B			54 728.931B	54 724.924	54 595.965	54 592.137b
17.5	54 666.947B	54 670.412			54 733.284	54 728.931B	54 598.833B	54 594.701B
18.5	54 667.512							
$J$	$Q_{11}(J)$			$Q_{22}(J)$				
0.5	54 690.004							
1.5				54 575.420				
2.5				54 577.572				

<sup>a</sup>Lines followed by B are observed as a single line and by *b* are observed as an incompletely resolved complex.

$$f(\nu', \nu'') = \frac{mc^2}{\pi e^2} \frac{1}{\tilde{N}(\nu'')} \int \sigma(\nu) d\nu, \quad (1)$$

in which  $\tilde{N}(\nu'')$  is the Boltzmann population of the absorbing vibrational level, and the integration of the cross-section  $\sigma(\nu)$  is performed over all of the rotational lines belonging to the  $(\nu', \nu'')$  band. The total cross-sections of observed lines for each branch are presented in Table III. Observations of the rotational lines are mostly limited to  $J \leq 16.5$ . The effects from higher  $J$  lines cannot be ignored. We extended the sum to  $J = 33.5$  by using the Boltzmann distribution and these value are presented in Table III as ‘‘Extended.’’ Yoshino *et al.*<sup>32</sup> made a similar correction for photoabsorption cross-section of Herzberg II bands of O<sub>2</sub>. For the  $P_{11}$

branch the individual line cross-sections could not be measured because of the blending, so only the total is given in Table III. As the highest  $J$ -value included in the integration is not known, we have not attempted to estimate the effect of the high- $J$  lines on this total. In the present case the rotational levels corresponding to values of  $J$  above 11.5 of  $C^2\Pi(\nu=1)$  are mixed with  $B^2\Pi(\nu=10)$ ,<sup>26</sup> and thus the mixing ratio must be taken into account to obtain the true band oscillator strength of the  $\delta(1,0)$  band. This analysis will be presented after the analysis of the  $\beta(10,0)$  band is completed.

Despite the mixing with the  $B^2\Pi(\nu=10)$  level, the perturbed oscillator strength of the  $\delta(1,0)$  band can be compared with previous published values. The sum of the integrated



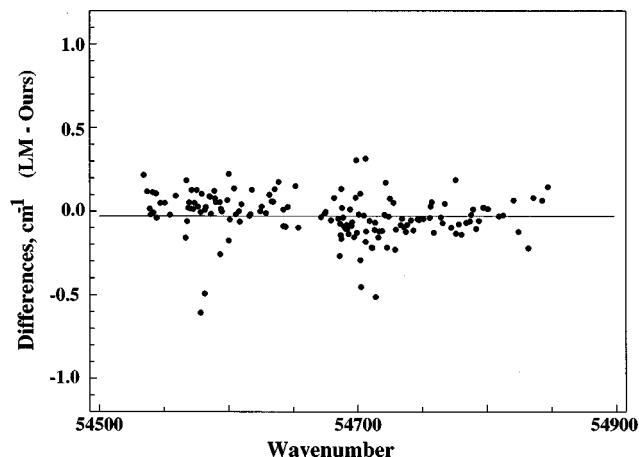


FIG. 2. Differences in the observed line positions between our results and Lagerqvist and Miescher (Ref. 26). The differences are given by the solid circles, and the solid horizontal line represents the average shift of  $-0.03 \text{ cm}^{-1}$ .

cross-sections of all observed rotational lines in Table III is  $4.79 \times 10^{-15} \text{ cm}^2 \text{ cm}^{-1}$ . The band oscillator strength  $f(1,0)$  determined from the above integrated cross-section is  $(5.4 \pm 0.3) \times 10^{-3}$ . This value agrees reasonably well with the previous values of  $6.0 \times 10^{-3}$  by Chan *et al.*,<sup>22</sup>  $5.8 \times 10^{-3}$  by Bethke,<sup>7</sup> and  $5.6 \times 10^{-3}$  by Cieslik,<sup>8</sup> but is 57% lower than the value of  $8.5 \times 10^{-3}$  reported by Guest;<sup>9</sup> the reason for this is not known. Our value is smaller than any of the previous values, but it is the only one derived from line-by-line measurements with a resolution comparable to the Doppler widths. Moreover, we were able to separate the lines of the

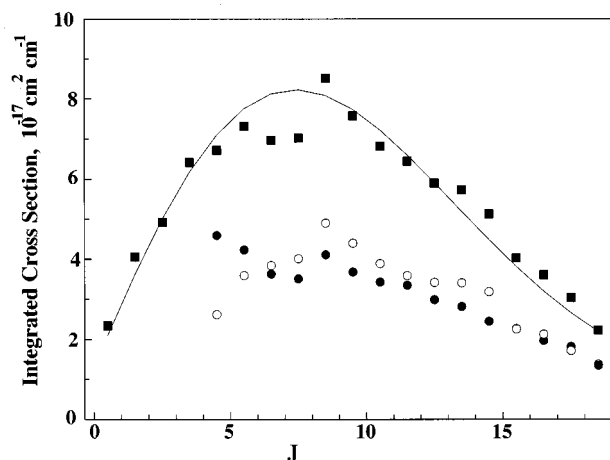


FIG. 3. The integrated cross-sections of the  $R_{11}$  branch lines. The lines with  $J > 4$  consist of two components,  $e$  and  $f$ , shown by solid and open circles, respectively. The total cross-sections are represented by solid squares.

$\delta(1,0)$  band from those of the overlapping  $\beta(10,0)$  band. This could not be done in the previous low resolution measurements, and it is possible that the blends may have led to overestimates of the band oscillator strength for the  $\delta(1,0)$  band by these authors. Bethke's value agrees with ours despite the possible error in his value pointed out by Callar and Pilling.<sup>13</sup>

#### IV. SUMMARY

This work provides the first absorption measurements of the  $\delta(1,0)$  band of NO free of problems arising from inad-

TABLE II. The term values and molecular constants of  $C(1) \ ^2\Pi$  level of NO,  $\text{cm}^{-1}$ .

$J$	$F_{1, \ ^2\Pi_{1/2}}$		$F_{2, \ ^2\Pi_{3/2}}$	
	$e$	$f$	$e$	$f$
0.5	54 690.000 ± 0.009	54 690.012 ± 0.009		
1.5	54 692.611 ± 0.013	54 692.629 ± 0.027	54 699.329 ± 0.016	54 699.353 ± 0.016
2.5	54 700.176 ± 0.014	54 700.193 ± 0.022	54 711.124 ± 0.006	54 711.120 ± 0.006
3.5	54 711.664 ± 0.020	54 711.702 ± 0.008	54 726.852 ± 0.019	54 726.538 ± 0.019
4.5	54 727.068 ± 0.024	54 727.084 ± 0.028	54 746.280 ± 0.009	54 745.819 ± 0.009
5.5	54 746.192 ± 0.015	54 746.656 ± 0.020	54 769.602 ± 0.006	54 768.939 ± 0.006
6.5	54 769.241 ± 0.116	54 769.883 ± 0.010	54 796.766 ± 0.010	54 795.878 ± 0.010
7.5	54 796.183 ± 0.011	54 797.021 ± 0.005	54 827.781 ± 0.006	54 826.643 ± 0.006
8.5	54 826.916 ± 0.006	54 828.001 ± 0.003	54 862.628 ± 0.007	54 861.219 ± 0.007
9.5	54 861.450 ± 0.011	54 862.818 ± 0.008	54 901.289 ± 0.006	54 899.582 ± 0.006
10.5	54 899.811 ± 0.013	54 901.473 ± 0.009	54 943.740 ± 0.009	54 941.707 ± 0.009
11.5	54 941.933 ± 0.015	54 943.907 ± 0.003	54 989.955 ± 0.008	54 987.556 ± 0.008
12.5	54 987.759 ± 0.008	54 990.094 ± 0.006	55 039.842 ± 0.007	55 037.077 ± 0.007
13.5	55 037.260 ± 0.014	55 039.975 ± 0.006	55 093.320 ± 0.005	55 090.180 ± 0.005
14.5	55 090.360 ± 0.013	55 093.439 ± 0.015	55 150.254 ± 0.015	55 146.730 ± 0.015
15.5	55 146.904 ± 0.005	55 150.380 ± 0.016	55 210.306 ± 0.018	55 206.484 ± 0.018
16.5	55 206.647 ± 0.013	55 210.461 ± 0.010	55 273.196 ± 0.029	55 269.042 ± 0.029
17.5	55 269.155 ± 0.050	55 273.245 ± 0.038		
18.5	55 333.718 ± 0.006	55 337.878 ± 0.005		
	$T_0$	54 690.155	± 0.017	
	$A$	3.556	± 0.078	
	$B_v$	1.94406	± 0.00062	
	$D_v \cdot 10^{-5}$	5.91	± 0.42	
	$A_D$	-0.0187	± 0.0050	
	$p$	-0.0189	± 0.0037	
	$q$	-0.01521	± 0.00020	

TABLE III. Integrated cross sections of lines of the  $\delta(1,0)$  band of NO in units of  $10^{-17} \text{ cm}^2 \text{ cm}^{-1}$ .<sup>a</sup>

$J$	$R_{11}(J)$		$R_{12}(J)$		$R_{21}(J)$		$R_{22}(J)$	
	$e$	$f$	$e$	$f$	$e$	$f$	$e$	$f$
0.5	1.79B				1.52			
1.5	3.52		1.31B		2.77B		1.22	
2.5	4.47		2.08B		1.91	1.64	0.58	1.33
3.5	6.28B		2.78B		2.88	1.54B	1.06b	2.17b
4.5	3.96B	2.32	1.90B	1.42	1.65	2.13B	1.82	1.63
5.5	3.65	3.23B	1.44b	1.25	2.35	2.29	1.97	1.75B
6.5	3.17B	3.63	1.68	1.67B	2.48	2.60	2.07	2.25B
7.5	3.14	3.62	1.31B	2.09b	2.51	2.12	2.21	1.97
8.5	3.70	4.58	1.24	1.52	2.71B	2.04	2.13	1.86B
9.5	3.29	3.99	1.02	1.46	2.00	1.67	2.10	2.09
10.5	3.08	3.40	1.00B	1.25	1.90	1.75		
11.5	2.87	3.23	0.79	0.89B	1.88	2.16B	1.76	1.18B
12.5	2.68	2.95	0.82	0.81	1.48	1.33	4.54	1.63
13.5	2.29	2.95	0.51	0.70	1.40	1.01	1.40B	1.31
14.5	2.17	2.50	0.52B	0.68	1.31	0.86	1.19B	1.33B
15.5	1.79	1.85	0.31	0.43	0.90	0.71	1.24	0.89B
16.5	1.52	1.68	0.73	0.09				
17.5	1.36	1.27						
18.5	1.79	0.57						
Total <sup>b</sup>	98.30		33.71		55.48		45.86	
Extended <sup>c</sup>	103.18		36.71		62.52		51.42	

$J$	$P_{11}(J)$		$P_{12}(J)$		$P_{21}(J)$		$P_{22}(J)$		$Q_{11}(J)$	$Q_{22}(J)$
	$e$	$f$	$e$	$f$	$e$	$f$	$e$	$f$		
0.5									1.35	
1.5										1.79
2.5			0.84		2.48B		2.34			1.16
3.5			1.66		2.83B		2.96			
4.5			1.96		1.77	3.62	3.42			
5.5			2.08		2.75	2.04	1.73	1.88		
6.5		0.99	1.02		2.29	2.10	2.40	1.50		
7.5		1.06	1.11		2.29	1.93	3.42	1.96		
8.5		1.07	1.38		2.39	2.47B	1.79	2.27		
9.5		1.08b	1.10		2.04	1.79B	1.83	1.98		
10.5		0.94B	0.92b		1.75	1.58	0.90B	1.69		
11.5		1.34	0.63B		1.41	1.11	0.89B	1.71		
12.5		0.67b	0.73B		1.54	1.86B	0.83B	1.46		
13.5		0.77b	0.55b		0.87	0.71B	0.96B	1.15		
14.5		0.72B	0.54B		0.59	0.55B	1.69b	0.59		
15.5		0.59B	0.71b		0.64	1.29B	1.04b	1.21b		
16.5		0.49B	0.27B		0.72B	1.01	1.27	1.42b		
17.5					0.29	0.57B	0.30	0.36B		
Total <sup>b</sup>	90.84		26.16		49.24		46.82		1.35	2.95
Extended <sup>c</sup>			28.49		52.62		49.85			

<sup>a</sup>Lines followed by *B* are observed as a single line and by *b* are observed as an incompletely resolved complex.<sup>b</sup>Total cross section for observed lines.<sup>c</sup>Total cross section after correction of higher  $J$  lines which are not observed. See text for detail.

equate spectral resolution, achieved by using the combination of a VUV FT spectrometer and a synchrotron radiation source. Accurate rotational line positions and term values as well as the photoabsorption integrated cross-sections are provided.

## ACKNOWLEDGMENTS

This work was supported in part by a NSF Division of Atmospheric Sciences Grant No. ATM-94-22854 to Harvard College Observatory, and by the NASA Upper Atmospheric Research Program under Grant No. NAG5-484 to the Smithsonian Astrophysical Observatory. We also acknowledge the

Paul Instrument Fund of the Royal Society for the development of the VUV-FT spectrometer. The FTS measurements at the Photon factory were made with the approval of the Photon Factory Advisory Committee (94G367). K.Y. thanks the Japan Society for the Promotion of Science for support.

<sup>1</sup>G. Brasseur and S. Solomon, *Aeronomy of the Middle Atmosphere* (Reidel, New York, 1984).

<sup>2</sup>T. Shimazaki, *Minor Constituents in the Middle Atmosphere* (Terra Scientific, Tokyo, 1985).

<sup>3</sup>M. Nicolet, *Ann. Geophys. (France)* **1**, 493 (1983).

<sup>4</sup>J. E. Frederic, A. J. Blake, and D. E. Freeman, *Handbook for MAP 8* (53 ICSC Scientific Committee on Solar Terrestrial Physics, Urbana, IL, 1983).

- <sup>5</sup>M. Nicolet and R. Kennis, *Planet. Space Sci.* **37**, 457 (1989).
- <sup>6</sup>K. Minschwaner, R. J. Salawitch, and M. B. McElroy, *J. Geophys. Res.* **98**, 10543 (1993).
- <sup>7</sup>G. W. Bethke, *J. Chem. Phys.* **31**, 662 (1959).
- <sup>8</sup>S. Cieslik, *Bull. Cl. Sci., Acad. R. Belg.* **63**, 884 (1977).
- <sup>9</sup>J. A. Guest and L. C. Lee, *J. Phys. B* **14**, 3401 (1981).
- <sup>10</sup>R. D. Hudson, *Rev. Geophys. Space Phys.* **9**, 305 (1971).
- <sup>11</sup>J. E. Murray, K. Yoshino, J. R. Esmond, W. H. Parkinson, Y. Sun, A. Dalgarno, A. P. Thorne, and G. Cox, *J. Chem. Phys.* **101**, 62 (1994).
- <sup>12</sup>K. Yoshino, J. R. Esmond, W. H. Parkinson, A. P. Thorne, J. E. Murray, R. C. M. Learner, G. Cox, A. S.-C. Cheung, K. W.-S. Leung, K. Ito, T. Matsui, and T. Imajo, *J. Chem. Phys.* **109**, 1751 (1998).
- <sup>13</sup>A. B. Callear and M. J. Pilling, *Trans. Faraday Soc.* **66**, 1886 (1970).
- <sup>14</sup>T. W. Dingle, P. A. Freedman, B. Gelernt, W. J. Jones, and I. W. M. Smith, *Chem. Phys.* **8**, 171 (1975).
- <sup>15</sup>O. Benoist D'Azy, R. Lopez-Delgado, and A. Tramer, *Chem. Phys.* **9**, 327 (1975).
- <sup>16</sup>K. Tsukiyama, T. Munakata, M. Tsukakoshi, and T. Kasuya, *Chem. Phys.* **137**, 315 (1987).
- <sup>17</sup>K. Tsukiyama, T. Munakata, M. Tsukakoshi, and T. Kasuya, *Chem. Phys.* **121**, 55 (1988).
- <sup>18</sup>T. Hikida, T. Suzuki, and Y. Moru, *Chem. Phys.* **118**, 437 (1987).
- <sup>19</sup>D. J. Hart and O. L. Bourne, *Chem. Phys.* **133**, 103 (1989).
- <sup>20</sup>C. Amiot and J. Verges, *Phys. Scr.* **25**, 302 (1982).
- <sup>21</sup>C. Amiot (private communication).
- <sup>22</sup>W. F. Chan, G. Cooper, and C. E. Brion, *Chem. Phys.* **170**, 111 (1993).
- <sup>23</sup>W. H. Parkinson, A. P. Thorne, G. Cox, P. L. Smith, and K. Yoshino, *Proc. SPIE* **2282**, 58 (1994).
- <sup>24</sup>J. W. Brault (private communication).
- <sup>25</sup>P. M. Dooley, B. R. Lewis, S. T. Gibson, G. H. Baldwin, P. C. Cosby, J. L. Price, R. A. Copeland, T. G. Slanger, K. Yoshino, A. P. Thorne, and J. E. Murray, *J. Chem. Phys.* **109**, 3856 (1998).
- <sup>26</sup>A. Lagerqvist and E. Miescher, *Helv. Phys. Acta* **31**, 221 (1958).
- <sup>27</sup>C. Amiot, R. Bacis, and G. Guelachvili, *Can. J. Phys.* **56**, 251 (1978).
- <sup>28</sup>J. T. Hougen, *NBS Monograph 115* (U.S. Government Printing Office, Washington, DC., 1970).
- <sup>29</sup>R. N. Zare, A. L. Schmeltekopf, D. L. Albritton, and W. J. Harrop, *J. Mol. Spectrosc.* **48**, 174 (1973).
- <sup>30</sup>C. Amiot, J.-P. Maillard, and J. Chauville, *J. Mol. Spectrosc.* **87**, 196 (1981).
- <sup>31</sup>G. Stark, J. W. Brault, and M. C. Abrams, *J. Opt. Soc. Am. B* **11**, 3 (1994).
- <sup>32</sup>K. Yoshino, J. R. Esmond, W. H. Parkinson, A. P. Thorne, R. C. M. Learner, and G. Cox, *J. Chem. Phys.* **111**, 2960 (1999).